ELSEVIER

Biochimica et Biophysica Acta 1554 (2002) 137–146

BIOCHIMICA ET BIOPHYSICA ACTA
BBA

www.bba-direct.com

Radicals associated with the catalytic intermediates of bovine cytochrome *c* oxidase

Peter R. Rich [a,*], Stephen E.J. Rigby [b], Peter Heathcote [b]

[a] *The Glynn Laboratory of Bioenergetics, Department of Biology, University College London, Gower Street, London WC1E 6BT, UK*
[b] *School of Biological Sciences, Queen Mary, University of London, Mile End Road, London E1 4NS, UK*

Received 8 January 2002; received in revised form 11 April 2002; accepted 3 May 2002

Abstract

Two radicals have been detected previously by electron paramagnetic resonance (EPR) and electron nuclear double resonance (ENDOR) spectroscopies in bovine cytochrome oxidase after reaction with hydrogen peroxide, but no correlation could be made with predicted levels of optically detectable intermediates (P_M, F and F$^{\cdot}$) that are formed. This work has been extended by optical quantitation of intermediates in the EPR/ENDOR sample tubes, and by comparison with an analysis of intermediates formed by reaction with carbon monoxide in the presence of oxygen. The narrow radical, attributed previously to a porphyrin cation, is detectable at low levels even in untreated oxidase and increases with hydrogen peroxide treatments generally. It is presumed to arise from a side-reaction unrelated to the catalytic intermediates. The broad radical, attributed previously to a tryptophan radical, is observed only in samples with a significant level of F$^{\cdot}$ but when F$^{\cdot}$ is generated with hydrogen peroxide, is always accompanied by the narrow radical. When P_M is produced at high pH with CO/O_2, no EPR-detectable radicals are formed. Conversion of the CO/O_2-generated P_M into F$^{\cdot}$ when pH is lowered is accompanied by the appearance of a broad radical whose ENDOR spectrum corresponds to a tryptophan cation. Quantitation of its EPR intensity indicates that it is around 3% of the level of F$^{\cdot}$ determined optically. It is concluded that low pH causes a change of protonation pattern in P_M which induces partial electron redistribution and tryptophan cation radical formation in F$^{\cdot}$. These protonation changes may mimic a key step of the proton translocation process.

Keywords: Cytochrome *c* oxidase; Hydrogen peroxide; Radical; EPR; ENDOR

1. Introduction

Structures of both mitochondrial and bacterial cytochrome *c* oxidases have been solved at atomic resolution [1,2] and provide many new insights on structure and mechanism. Nevertheless, major questions remain as to the chemical nature of important intermediates and the sites that are involved in key protonation reactions. The catalytic cycle of oxygen reduction is thought to include "peroxy" (P) and "ferryl" (F) intermediates (cf. Ref. [3]). These species were first described in reversed electron transfer studies using coupled mitochondria [4,5], and have since been observed in the forward reaction of fully reduced cytochrome *c* oxidase [6,7] and other haem-copper oxidases [8,9] with oxygen. In the visible region P and F are characterised by distinct peaks at 607 and near 580 nm, respectively, but in the Soret region, both exhibit a similar red shift relative to the oxidised (O) state [10]. P and F can be formed from O by addition of dioxygen together with two or three reducing equivalents, respectively [11]. Spectroscopic features of F are characteristic of a Fe(IV)=O Cu_B(II) ferryl compound, but those of P do not have a clear precedent and, originally, were interpreted as a ferric–peroxide structure. However, a number of independent lines of investigation provide very strong evidence to support the suggestion [12,13] that the O—O bond is already broken in P, so that this species also has an $Fe^{4+}=0^{2-}$ ferryl structure. This evidence includes magnetic circular dichroism (MCD) [14], Raman data on the

Abbreviations: O, fully oxidised; R, binuclear centre-reduced; P, 607 nm species; P_M, a stable P species formed when mixed-valence enzyme reacts with oxygen; P_R, a transient P species with one more electron in the vicinity of the binuclear centre in comparison to P_M; F$^{\cdot}$, a 575 nm ferryl species that is isoelectronic with P_M; F, a 580 nm ferryl species that is isoelectronic with P_R; EPR, electron paramagnetic resonance; ENDOR, electron nuclear double resonance; ΔHptp, line width peak-to-peak of first derivative EPR spectrum; rf, radiofrequency

* Corresponding author. Tel./fax: +44-20-7679-7746.
E-mail address: PRR@UCL.AC.UK (P.R. Rich).

0005-2728/02/$ - see front matter © 2002 Elsevier Science B.V. All rights reserved.
PII: S0005-2728(02)00228-1

iron–oxygen stretch frequency [15–17] and the release of half of the labelled oxygen as water when P is formed with O_2^{18} [18].

Species related to P and F can be formed by alternative means. At high pH, incubation of oxidised enzyme with CO and oxygen results in a 607 nm species [19,20], presumably by a two-electron reduction by CO, followed by reaction of the mixed-valence product with oxygen. This species has been termed P_M to distinguish it from a related 607 nm P state, P_R, that is formed transiently when oxygen reacts with the fully reduced enzyme [21–24]. P_R differs from P_M in that the binuclear centre contains an additional electron that is donated by haem *a* [6,25].

Oxidised enzyme can also react with H_2O_2 to produce related species. Extents, rates of reaction, and the ratio of the forms, depend on pH and H_2O_2 concentration [12,26,27]. At high pH, the reaction initially produces a 607 nm species that reacts with a second H_2O_2 to form a 580 nm product. These appear to be identical to P_M and F, respectively. However, a third species can be formed by reaction with a single H_2O_2 at low pH, or by lowering the pH of a sample of P_M that has been formed with CO/O_2 at high pH [28]. This species is anomalous in that it is isoelectronic with the 607 nm P_M state but has a visible absorption band similar to that of F [28]. Because of its supposed similarity to F, it was termed F′ [14,29] or $F^{\cdot}$ [30].

Formation of ferryl species from the oxidised state requires input of three electrons. For the F species, these are provided by external reductant. In the case of P_M and $F^{\cdot}$, however, only two electrons have been provided from external sources. The third electron must be provided from within the protein, raising the likelihood that radical species will be formed at the donor sites. Two electron paramagnetic resonance (EPR)-detectable radical signals were indeed formed on incubation of bovine cytochrome *c* oxidase with H_2O_2 under various conditions [12,28]. These were assigned to porphyrin and tryptophan cation radicals [31], but no clear correlation could be made between the level of either radical and the calculated level of any specific intermediate in the same sample [28]. Furthermore, in an equivalent study of *Paracoccus denitrificans* cytochrome *c* oxidase [32] a quite different radical, identified as a tyrosine, was formed after reaction with H_2O_2. This radical has been suggested to reside on a novel tyrosine that is covalently linked to a histidine ligand of Cu_B [33,34] and a mechanistic role for a radical state of this tyrosine has gained considerable further support [32,35–38]. In this paper, we clarify the origins of the two EPR-detected radicals that can be formed in bovine oxidase and assess their relation to previously reported species and their possible roles in the catalytic cycle.

2. Materials and methods

2.1. Preparation of bovine heart oxidase

Cytochrome *c* oxidase was prepared by a procedure [39], which yields ‘fast’ enzyme with monophasic cyanide binding kinetics and a characteristic Soret maximum at 424 nm. It was quantitated optically from the dithionite-reduced minus oxidised difference spectrum using an extinction coefficient of $\Delta\varepsilon_{606-621\ nm} = 25.7\ mM^{-1}\ cm^{-1}$ [10].

2.2. Optical spectroscopy and component deconvolution

Optical spectra and multi-wavelength kinetics were monitored at room temperature in the same sample using a single-beam instrument built in-house. A modification was made so that the beam could be focussed through samples in EPR tubes before freezing. This enabled recording of quantitative optical spectra of samples in the EPR tubes during the course of the reactions so that levels of species generated could be quantitated. In all cases, absolute spectra versus buffer were first recorded in the visible region, allowing the effective path length to be calculated from the size of the 598 nm peak. This was used to quantitate the levels of intermediates formed subsequently on treatment with H_2O_2 or CO/O_2. The levels of 607 nm (P) and 580/575 nm (F and $F^{\cdot}$) were deconvoluted using the matrix of extinction coefficients given in Table 1. The relative amounts of F and $F^{\cdot}$ in their combined total were assumed from the known behaviour of oxidase [28] under the specific conditions used for each sample.

Table 1
Extinction coefficients used for quantitation of mixture of states of cytochrome oxidase

Wavelength (nm)[a]	425	598	439–414	436–414 434–413[b]	575/580–630[b]	607–630
	$mM^{-1}\ cm^{-1}$	$mM^{-1}\ cm^{-1}$	$mM^{-1}\ cm^{-1}$	$mM^{-1}\ cm^{-1}$	$mM^{-1}\ cm^{-1}$	$mM^{-1}\ cm^{-1}$
Oxidised	160	23.8	–	–	–	–
P *minus* O	–	–	45	–	1.9	10.4
$(F + F^{\cdot})$ *minus* O[b]	–	–	–	50	4.0	1.9

[a] Data are derived from spectra reviewed in Ref. [10].

[b] Peak positions of $F^{\cdot}$ are blue-shifted in comparison to F. The total amount of $(F + F^{\cdot})$ was estimated by measurement at the peak position, assuming equal peak/trough extinction coefficients for F and $F^{\cdot}$.

2.3. Electron paramagnetic resonance and electron nuclear double resonance spectroscopies

Continuous-wave EPR spectra were recorded on a Jeol RE1X spectrometer fitted with an Oxford Instruments cryostat. Conditions of measurement were as indicated in the figure legends. Spin intensities were quantitated by double-integration and calibrated against a sample of known concentration of photo-oxidised P700 in Photosystem I particles from spinach, prepared using Triton X-100 as described previously [40]. The concentration of P700 was determined optically from an ascorbate-reduced *minus* ferricyanide-oxidised difference spectrum using an extinction coefficient of 64 mM^{-1} cm^{-1} at 703 nm. $P700^{+}$ was generated by illuminating the sample in the EPR tube for 60 s and freezing in liquid nitrogen under illumination. Electron nuclear double resonance (ENDOR) spectra were obtained at X-band using a Bruker ESP 300 EPR spectrometer. Acquisition conditions are given in the figure legends.

2.4. Net proton changes

The method was based on that described in Ref. [41] to determine protonation properties of other oxidase intermediates. Measurements were made with a single beam spectrophotometer built in-house that was capable of sequential measurement of multiple wavelengths. Cytochrome oxidase was diluted to 3.65 μM in a medium of 50 mM potassium sulfate which contained 0.05% lauryl maltoside and 50 μM bromocresol purple. pH was adjusted to 5.9 and the reaction was initiated by addition of 100 μM H_2O_2. Under these conditions, the reaction results in formation primarily of $F^{\cdot}$, which was monitored quantitatively at the wavelength pair 434–413 nm [28] and with an extinction coefficient of 50 mM^{-1} cm^{-1} (assumed to be the same as that for F at 436–414 nm [10]). Proton changes in the medium were determined from the absorbance change of bromocresol purple at 549–529 nm and were calibrated by additions of aliquots of KOH and HCl.

2.5. H_2O_2 solutions

Serial dilutions of a 30% w/v (8.8 M) stabilised H_2O_2 stock were made with double-distilled water. Diluted solutions were kept on ice and used within 4 h.

3. Results

3.1. Optical and EPR quantitation of species formed with H_2O_2

Fig. 1 (left panel) shows typical visible difference spectra versus the untreated oxidised state of the mixtures of intermediates formed in bovine oxidase samples in EPR tubes at room temperature after reaction with hydrogen peroxide under various conditions. The levels of intermediates in each of these samples were deconvoluted as described in Materials and methods. The samples were frozen in liquid nitrogen immediately after the optical spectra were recorded and the corresponding EPR spectra of the frozen samples are also shown (right panel). At pH 6 and after treatment with 0.5 mM H_2O_2 for 3 min (traces A), the sample contained 55% (F plus $F^{\cdot}$), together with around 20% P_M and because of the low pH, it is assumed that the majority of the 575/580 nm species is $F^{\cdot}$. The corresponding EPR spectrum had the same mixture of broad (ΔHptp = 45 G) and narrow (ΔHptp = 12 G) radicals as found previously for similar conditions [28,31]. At pH 8.5 and after treatment with 0.5 mM H_2O_2 for 5 min (traces B) the sample contained 40% (F plus $F^{\cdot}$), together with 30% P_M and, because of the high pH, it is assumed that the majority of the 575/580 nm species in this sample is F. The corresponding EPR spectrum in Fig. 1B predominantly showed the narrow radical form. At pH 8.5 and after treatment with 50 μM H_2O_2 for 4 min (traces C) the sample contained around 35% of the P state with less than 10% of the (F plus $F^{\cdot}$) forms. Its corresponding EPR spectrum in Fig. 1B exhibited mostly the narrow radical form.

3.2. Optical and EPR quantitation of species formed with CO/O_2

Fig. 1 (traces D) also shows a similar analysis of a sample which had been exposed to carbon monoxide in the presence of oxygen for 3 min at pH 8.5, followed by lowering of the pH to 6.2 after the CO had been rigorously removed (cf. Ref. [28]). The optical spectrum showed predominantly a species absorbing around 575 nm with only a faint trace (< 5% occupancy) of the 607 nm P_M form. From previous studies [28], it is expected that this species is $F^{\cdot}$ rather than F, a supposition supported by the fact that the peak was at 575 nm rather than the 580 nm position characteristic of F [42]. Quantitation relative to the absolute spectrum indicated that it was present at around 70% occupancy. The corresponding EPR spectrum in Fig. 1 exhibited a broad radical species (ΔHptp = 35 G) with only a small amount of a narrower radical whose amount was similar to that seen in untreated samples (not shown).

The behaviour of a more concentrated (40 μM) sample that was subjected to CO/O_2 and low pH was investigated in more detail in Fig. 2. Quantitation of the spectrum in the presence of CO/O_2 at pH 8.5 relative to the absolute spectrum (not shown) indicated that the P_M state formed quantitatively at pH 8.5. Provided that CO/O_2 remained in the sample, the P_M was indefinitely stable and no 575/580 nm species appeared. If the pH was dropped to 6.5 by addition of a small amount of concentrated buffer while CO was still present, the amount of P_M decreased as it converted back to O, but no 575/580 nm species accumulated (data not shown). This is consistent with our previous finding of the extent of formation of P_M with CO/O_2 as a function of pH

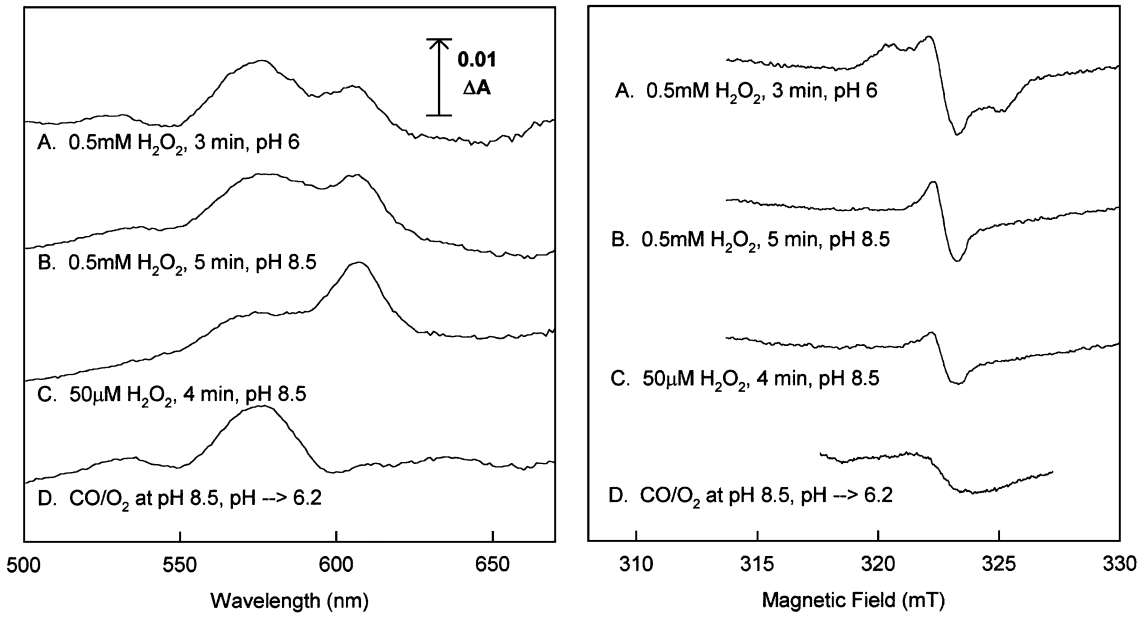

Fig. 1. Optical and EPR spectra of species formed after reaction with H_2O_2 or CO/O_2. Cytochrome oxidase was diluted to a concentration of 14 μM in a buffer of 10 mM potassium phosphate at pH 8.5 or 6 and containing 0.05% w/v dodecyl maltoside. The sample was placed in an EPR tube and an absolute spectrum was recorded at room temperature versus a buffer blank, from which an effective path length of 0.18 cm could be calculated for this matched set of EPR tubes. Hydrogen peroxide was added at the concentrations shown (traces A–C) and optical difference spectra versus the absolute spectrum were recorded after the times indicated. The samples were then frozen immediately in liquid nitrogen and the corresponding EPR spectra were taken. The CO/O_2-treated sample (traces D) was initially at pH 8.5. It was removed from the EPR tube and bubbled with CO for 30 s, after which time P_M had formed quantitatively (not shown). CO was then removed by vacuum evacuation and argon bubbling (see Results) before being returned to the EPR tube. A pH jump to 6.2 (measured in the thawed sample after recording spectra) was initiated by addition of a final concentration of 100 mM potassium-MES at pH 5.6. The optical spectrum (trace D) was recorded versus the absolute spectrum after 90 s incubation at room temperature, after which time the sample was frozen and the corresponding EPR spectrum was recorded. EPR conditions were: microwave power 200 μW (spectra A–C) or 1 mW (spectrum D); modulation amplitude, 0.5 mT; temperature, 45 K. Spectra are each the sum of four scans.

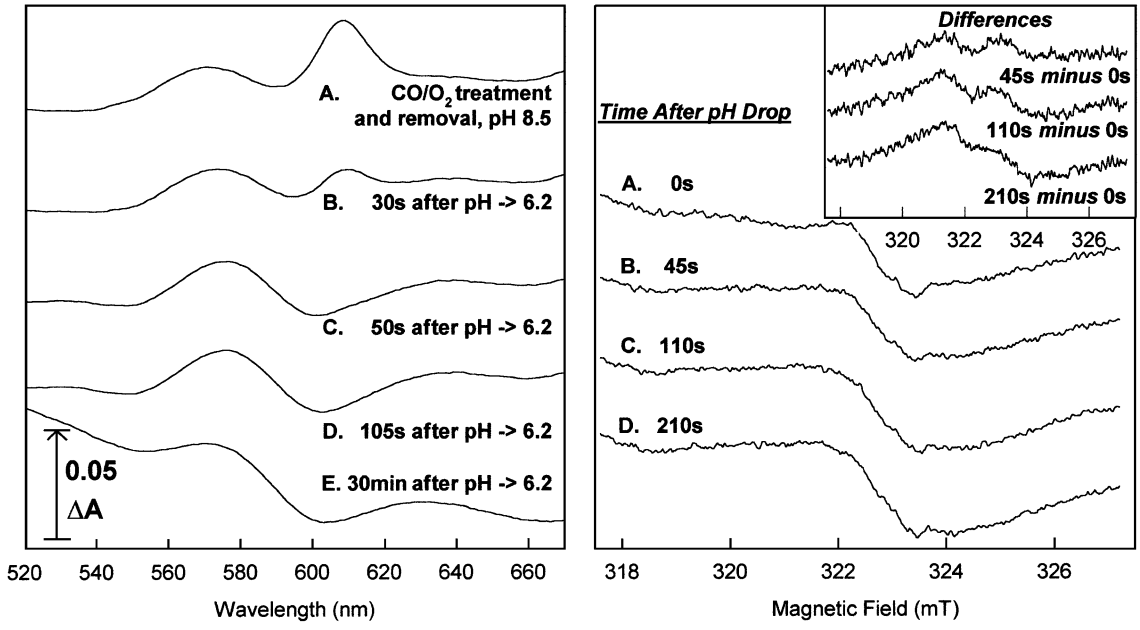

Fig. 2. Kinetics of formation of optical and EPR species formed with CO/O_2. Cytochrome oxidase was diluted to a concentration of 40 μM in a buffer of 10 mM potassium phosphate at pH 8.5 and containing 0.05% w/v dodecyl maltoside. An absolute spectrum was recorded, from which an effective path length of 0.15 cm was calculated for this matched set of EPR tubes. Samples were treated with CO/O_2, CO was removed and pH dropped to 6.2 as in Fig. 1. In this case, individual samples were used and incubated for various times after initiation of the pH drop to 6.2, at which point they were analysed optically or frozen for EPR analysis. EPR conditions were: microwave power 200 μW; modulation amplitude, 0.5 mT; temperature, 45 K. EPR spectra are each the sum of four scans.

[28]. Presumably, lowering of pH accelerates the reaction of P_M with CO to regenerate the oxidised form, so that the steady state occupancy of P_M is lowered as the pH decreases. Any $F^{\cdot}$ formed directly from P_M must also react with CO, again to form O, but at a rate far greater than its rate of formation so that none accumulates. If, however, the CO is removed rigorously before the pH drop, the P_M species can convert spontaneously into an $F^{\cdot}$ form that is relatively stable [28]. In order to achieve sufficient depletion of CO, the CO/O_2-treated sample was transferred to a Thunberg tube, degassed five times by evacuation with a water pump, and then bubbled with argon for 30 s before being returned to the EPR tube. The visible difference spectrum versus the untreated oxidised state (Fig. 2 left, trace A) indicated that P_M was still present, but had diminished to approximately 50% occupancy when quantitated by comparison with its absolute oxidised spectrum, again with no indication of 575/580 nm species. The pH was then dropped to pH 6.2 and optical spectra were recorded sequentially (traces B–E). The P_M converted to $F^{\cdot}$ within a few minutes and remained relatively stable over tens of minutes (trace E). Fig. 2 (right) shows the EPR spectra of equivalent samples that were frozen after different incubation times following the pH drop to 6.2. Formation of the pure P_M state with CO/O_2 at pH 8.5 did not produce any radicals (Fig. 2 right, trace A) that were additional to the small level found in untreated control samples (not shown), consistent with previous reports [12,28]. However, upon lowering the pH of the CO-free sample to pH 6.2, the broad radical component appeared over the course of a few minutes (Fig. 2 right, traces B–D). Its appearance is seen most clearly in the inset, which shows EPR spectra of the incubated samples after subtraction of the EPR spectrum of the trace A sample. The time courses for interconversion of the 607/575 nm forms and for formation of the broad EPR-detected radical were derived from these data and are plotted in Fig. 3, and within experimental error, have the same rate constant of 0.03 s^{-1}.

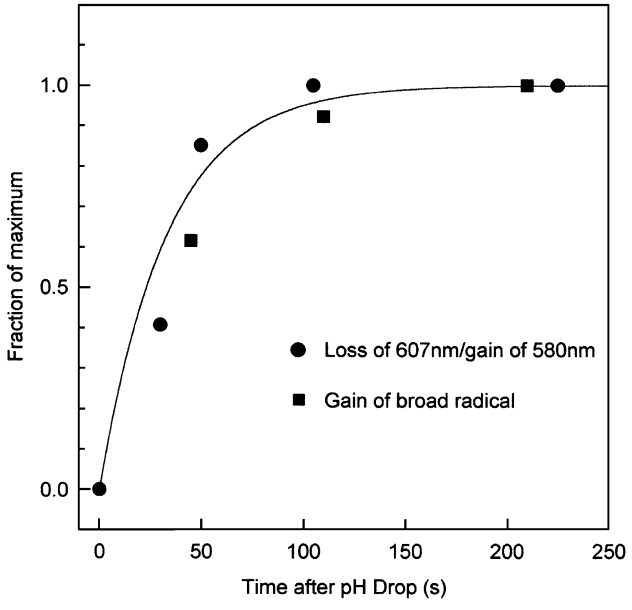

Fig. 3. Time courses for optical species interconversion and broad radical appearance. Loss of 607 nm/gain of 575 nm species and appearance of the broad radical were quantitated from the data of Fig. 2. Values were normalised to maximum amounts and plotted versus incubation times at pH 6.2. The curve shows an exponential decay of $k = 0.03\ s^{-1}$ for comparison.

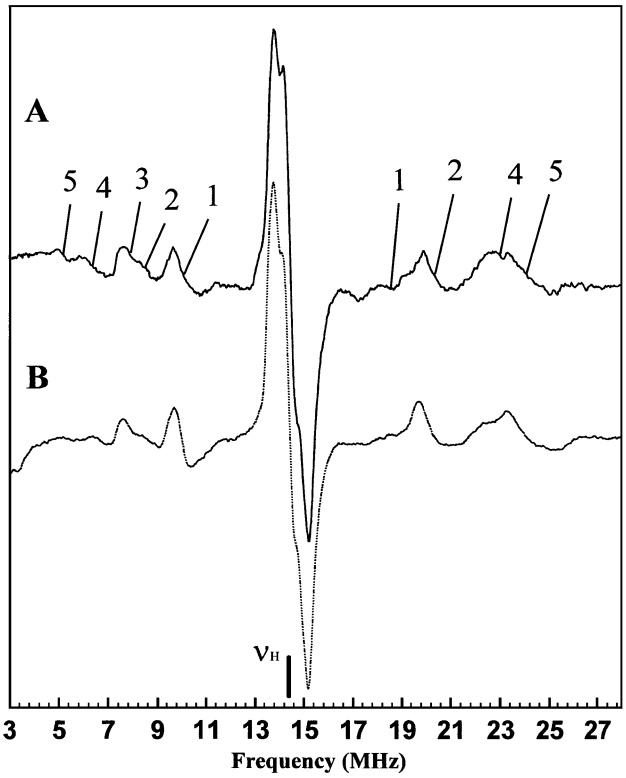

Fig. 4. ENDOR spectrum of the broad radical formed at low pH after CO/O_2 treatment. Spectrum A is an ENDOR spectrum of the 40 μM cytochrome oxidase sample used to produce the EPR spectrum D in the figure. Spectrum B (a reproduction of trace b from Fig. 2 of Ref. [31]) is shown for comparison and is of a sample of cytochrome oxidase that had been treated with 1 mM hydrogen peroxide at pH 6.5 for 3 min before freezing. ENDOR conditions were, for spectrum A: microwave power 15.9 mW, rf power 125 W, rf modulation depth 177 kHz, average of 60 scans, temperature 12 K; for spectrum B: microwave power 24 mW, rf power 100 W, rf modulation depth 140 kHz, average of 60 scans, temperature 12 K.

Quantitation of the EPR spectrum of the broad radical that formed at pH 6.2 in EPR sample D in Fig. 2 gave approximately 0.6 μM spins. However, estimation of the level of $F^{\cdot}$ from the optical spectra showed that it was present at about 50% occupancy, i.e. 20 μM. Hence, the

Table 2
Hyperfine coupling constants and assignments

Feature	Hyperfine coupling (MHz)	Assignment
1	8.6	ring C(5)H
2	11.4	$\beta-CH_2$ A_{iso}
3	13.0	ring C(7)H
4	15.2	ring C(2)H
5	18.8	$\beta-CH_2$ A_{iso}

Values were derived from spectrum A in Fig. 4.

broad radical associated with F· is observable by EPR only to 3% of the level of F·, assuming that the entire 575 nm feature is attributed to F·.

3.3. ENDOR analysis of the broad radical formed with CO/O_2

An ENDOR spectrum of the sample used to produce the broad radical shown in trace D of Fig. 2 was recorded. This spectrum displayed the same general features and proton hyperfine couplings (Fig. 4 and Table 2) as those reported previously for the broad EPR radical generated at pH 6.5 with hydrogen peroxide [31]. Furthermore, as also observed for the H_2O_2-generated species, the spectrum of the CO/O_2-generated form could not be obtained above 20 K and no other ENDOR spectrum was detected at the higher temperatures that were employed to obtain the ENDOR spectrum of the narrow porphyrin cation radical that is also produced with hydrogen peroxide.

3.4. Protonation changes associated with formation of F·

In order to further elucidate the nature of the chemical change occurring in the change from O to F·, the net change of protonation state of the oxidase during this transition was determined. The method was the same as that used previously to show that the P_M and F forms have two and three protons, respectively, more than O [41]. The experiment was performed at pH 6.2 and in the presence of bromocresol purple (pK 6) to monitor net proton changes. Kinetics of formation of F· on addition of 100 μM H_2O_2 were monitored at the wavelength pair 434–413 nm and its extent was quantitated with an assumed extinction coefficient of 50 $mM^{-1}\cdot cm^{-1}$. Proton changes in the medium were monitored at 549–529 nm (which minimised interference from changes of cytochrome oxidase) and calibrated with aliquots of KOH and HCl. A typical result is shown in Fig. 5. F· formed almost quantitatively over a time course of about 20 s. A small pH drop occurred immediately upon addition of the H_2O_2. However, net proton release/uptake in the medium during the time course of conversion of O to F· was <0.2 H^+/oxidase. Hence, the two protons of the reactant H_2O_2 are not released and must remain bound in F·.

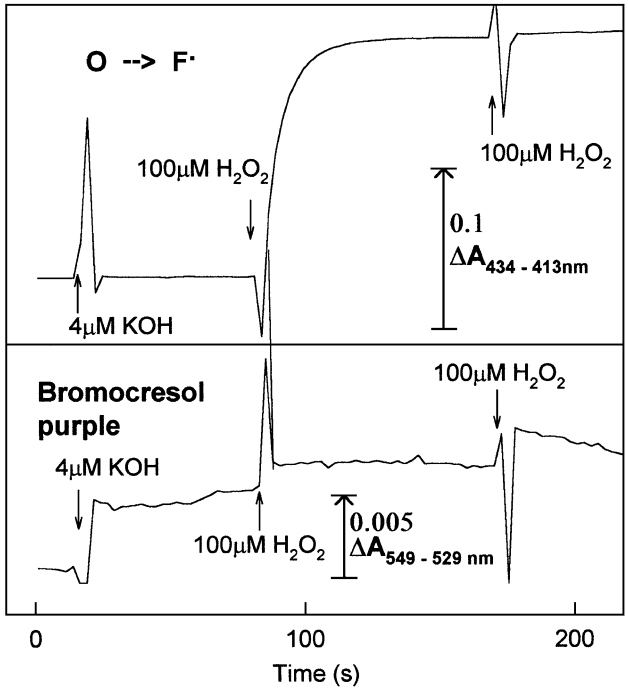

Fig. 5. Protonation changes associated with the formation of F· from the oxidised form of bovine oxidase. Cytochrome oxidase was diluted to 3.65 μM in a medium of 50 mM potassium sulfate which contained 0.05% lauryl maltoside and 50 μM bromocresol purple. pH was adjusted to 6.2 and an aliquot of KOH was added to calibrate the bromocresol purple changes at 549–529 nm. The reaction was initiated by the addition of 100 μM H_2O_2. F· formation was monitored at the wavelength pair 434–413 nm and net proton changes in the medium were determined from the absorbance change of bromocresol purple at 549–529 nm. Finally, a second aliquot of 100 μM H_2O_2 was added to confirm that the reaction was complete.

4. Discussion

Since both P_M and F· have only two reducing equivalents more than the oxidised enzyme, an additional electron is required from a site other than the binuclear centre metals in order to form the $Fe^{4+}=O^{2-}$ ferryl state. One proposed source for this additional electron is the unusual covalently linked tyrosine–histidine pair within the binuclear centre [33,34], which could form a radical species and which could be of significance in the coupling mechanism [35,36,43,44]. In a study of intermediates formed in *P. denitrificans* cytochrome *c* oxidase after reaction with H_2O_2 at low pH, a radical species, attributed to a tyrosine, was indeed found [32]. Furthermore, a radical state of tyrosine Y244 was trapped by iodination of the P_M state of bovine oxidase [37] and a possible tyrosyl radical with a Raman band at 1489 cm^{-1} was proposed to be associated with the equivalent of the P_M state in cytochrome *bo* of *Escherichia coli* [38]. Nevertheless, EPR spectra of P_M generated by CO/O_2 treatment do not exhibit a detectable radical ([12,28] and this study). Most likely, this is because of spin coupling within the tyrosine–histidine–Cu_B^{2+} system that renders the radical state EPR-silent [12].

When bovine oxidase reacts with hydrogen peroxide, two distinct radicals can be detected, albeit at low occupancy, and these were assigned by ENDOR spectroscopy to porphyrin cation and tryptophan cation radicals [31]. However, radicals are formed with hydrogen peroxide treatments even when the sole optically detectable product of the reaction is P_M (Fig. 1, traces C), whereas none are evident (other than a small background signal seen in untreated enzyme) when P_M is formed with CO/O_2 (Fig. 2, traces A and Ref. [12]). This requires explanation since the P species formed with CO/O_2 or with H_2O_2 appear otherwise to be

identical [28]. A further complication with the H_2O_2 reaction products is that no clear correlation could be found between the level of either radical and the levels of P_M, F, or $F^{\cdot}$ that were predicted to be present by extrapolation from known kinetic behaviour of much lower concentrations of oxidase in optical cuvettes [28]. However, it is possible that kinetic behaviour of the system at the higher protein concentrations used for EPR samples could vary significantly from that observed at low concentrations, obscuring the correlations between signals. Hence, in the present study, the reaction products formed in the EPR tubes were quantitated directly by visible spectroscopy and this allowed a more precise comparison of the optically and EPR-detectable species. As can be seen from Fig. 1, however, there was still no correlation between radicals and specific intermediates after the H_2O_2 treatments. The narrower porphyrin radical is present to some extent in all H_2O_2-treated samples, regardless of whether the major product is P_M, F or $F^{\cdot}$. However, in samples treated with CO/O_2, the narrow radical was not evident at all above the low level found even in untreated oxidase. Hence, it is concluded that the narrow porphyrin radical is the product of a side-reaction with hydrogen peroxide and is not a component of a catalytic intermediate. It might be noted that this radical does not form when H_2O_2 is reacted with cyanide-ligated oxidase samples [28]. Hence, its formation does require an initial reaction of hydrogen peroxide with the binuclear centre in order to produce the active oxidant. We have found (Scerri and Rich, unpublished) that incubation of bovine cytochrome oxidase with millimolar concentrations of H_2O_2 leads to irreversible loss of cytochrome *c* oxidase activity (15–40% loss over 30 min at room temperature), confirming the idea that damaging side-reactions can occur and highlighting the need for care in the use of hydrogen peroxide for quantitative mechanistic studies.

In contrast to the above, reaction with CO/O_2 provides a positive correlation of the level of a broad radical with the level of $F^{\cdot}$ determined optically. Its ENDOR spectrum displays the same general features, temperature dependency and hyperfine couplings (Fig. 4 and Table 2) as those reported previously for the broad radical generated at pH 6.5 with H_2O_2 [31]. Therefore, it is assigned to the same tryptophan cation radical that is exchange coupled to the haem iron. The signal is weaker than that obtained with hydrogen peroxide and so higher radiofrequency (rf) modulation depth (177 compared to 140 kHz) and rf power (125 compared to 100 W) were employed. In addition, the optimum microwave power for ENDOR spectroscopy was slightly changed by the conditions used for its generation (15.9 mW at 12 K compared to 24 mW in the previous study of the H_2O_2-generated species). This suggests a slight decrease in electron spin relaxation times and may be due to the absence of the porphyrin cation radical that is always formed with H_2O_2 treatments. Quantitation indicates that it is EPR-detectable at a level of only 3% of that of optically detectable $F^{\cdot}$.

Overall, assuming that both P_M and $F^{\cdot}$ are ferryl species and have a radical, we interpret these data as follows: in the P_M state, the radical resides wholly on the tyrosine–histidine–Cu_B structure and, as suggested elsewhere [12], is EPR-silent due to spin coupling. Low pH induces conversion to the isoelectronic $F^{\cdot}$ and involves electronic redistribution such that a part of the radical migrates to a tryptophan to produce an EPR-detectable tryptophan cation radical. Three tryptophans are very close to haem a_3/Cu_B, located just above the metals towards the positive phase (Fig. 6). All three are highly conserved and W126 was suggested to be the most likely candidate from spectroscopic and distance considerations [31], although a distribution over several residues is also possible. Dutton

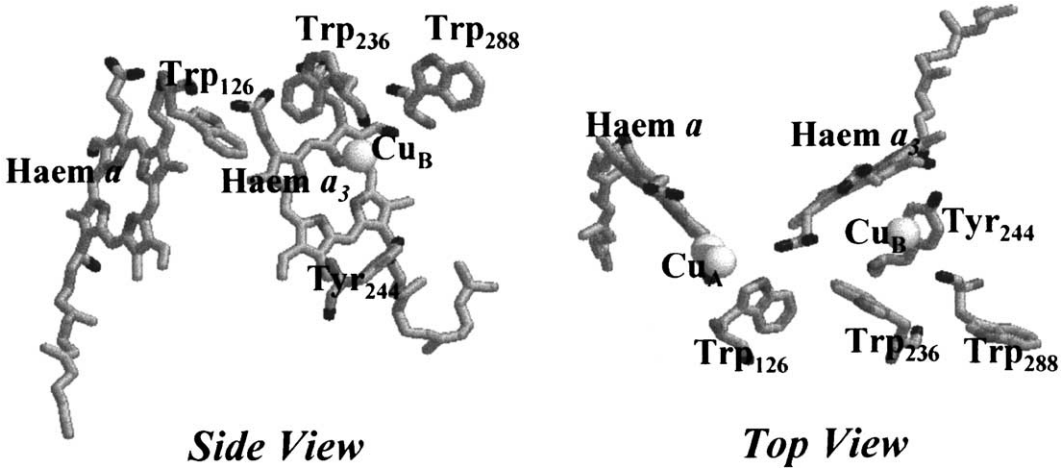

Fig. 6. Tryptophan residues close to the binuclear centre in bovine cytochrome *c* oxidase. The figure was drawn from PDB file 1 OCC coordinates [1] using RasMol software. Numbers refer to the bovine subunit I sequence.

(personal communication) has estimated that electron transfer between all three tryptophans and the binuclear centre can take place with rate constants in excess of 10^8 s^{-1} and so all are easily kinetically competent in charge redistribution within the lifetime of an intermediate.

The data in Fig. 5 shows that there is no significant uptake/release of protons in the medium when $F^{\cdot}$ is formed from O with hydrogen peroxide at pH 6.2. Hence, the two protons of hydrogen peroxide must remain bound within the protein in $F^{\cdot}$. Both protons are also retained within the protein when the P_M is generated from O [41]. Provided that the protonation state of groups involved in intermediate conversion remain the same at low and high pH, this means that P_M and $F^{\cdot}$ also have the same number of protons so that $F^{\cdot}$ obeys the same charge compensation rule [45] as the other intermediates. This is in accord with Fabian and Palmer [46] who also noted recently that reaction of O with H_2O_2 at low pH did not result in any net proton change in the medium. However, they also found [46] that conversion of P_M to a 580 nm species by lowering pH involves uptake of a proton, which would imply that P_M and their 580 nm product (which we would interpret to be $F^{\cdot}$) differ by one proton so that electroneutrality is not maintained in $F^{\cdot}$. These data could be reconciled if O becomes protonated to a form $O(H^+)$ at low pH and this proton remains bound in $F^{\cdot}$. In this way, conversion of P_M to $F^{\cdot}$ by lowering pH would lead to uptake of a proton as observed in Ref. [46], whereas formation of P_M from O [41] and formation of $F^{\cdot}$ from $O(H^+)$ (above and in Ref. [46]) would not. Such pH-dependent protonation of critical groups influenced by the binuclear centre might be consistent with the report of Capitanio et al. [47] that net proton uptake on reduction of the binuclear centre decreases at low pH. Baker and Palmer [48] previously provided spectroscopic evidence that O does indeed have pH-dependent forms and have suggested [46] that they are responsible for the pH-dependent change of reaction with hydrogen peroxide. However, it is not clear whether the small optical changes observed in Ref. [48] were due to a pH-dependent equilibrium of reactive forms of O or were instead caused by some conversion to the 'resting' form of O which has very large optical changes and which does not react with hydrogen peroxide [49]. The experiments in Ref. [46] relating to a proton uptake in conversion of P_M to $F^{\cdot}$ may also require further considerations: their slope of -1 in a plot of log conversion rate versus pH clearly shows that a single protonatable group controls the reaction, as they note, but this in itself does not mean that a proton remains bound in the reaction. The fact the P_M to $F^{\cdot}$ change could not be reversed by raising pH [28,46] also raises questions as to whether the conversion involves a simple equilibrium controlled by proton binding. Furthermore, direct measurement of proton changes in the medium when P_M was converted to $F^{\cdot}$ in Ref. [46] required subtraction of a background of extensive, heterogeneous surface protonation changes that must occur when O is subjected to the same pH drop. Such a large background subtraction could well distort the quantitative assessment of protonation events associated specifically with the P_M to $F^{\cdot}$ conversion. Recent work of Pecoraro et al. [42] also relates to these questions. They showed that mutation of the K channel prevents the low pH pathway for $F^{\cdot}$ formation and concluded that the K channel is involved in the controlling protonation process. Interestingly, they also showed that prolonged incubation of the mutant at low pH failed to promote the $F^{\cdot}$ pathway. They concluded that if a net proton uptake does actually occur in forming $F^{\cdot}$, this must be taken up *after* or *during* reaction with peroxide.

Taking all of the above into account, it is not possible at present to distinguish definitively whether the O state has a key site that becomes protonated at low pH, nor to establish whether P_M and $F^{\cdot}$ differ in their net degree protonation. Further experiments will be required to resolve this crucial point.

If indeed P_M and $F^{\cdot}$ have the same net degree of protonation, as would be expected if both adhere to the electroneutrality rule and as at least suggested from the simple measurements of proton changes in the medium after reactions with hydrogen peroxide, then low pH must act as a catalyst to promote a kinetically hindered equilibrium rather than being involved in shifting a pH-dependent equilibrium. Hence, any stable protonation associated with the $P_M/F^{\cdot}$ transition should be accompanied by the concurrent loss of a proton from elsewhere in the structure in order to maintain overall electroneutrality. In this case, it would be tempting to propose that the proton loss would occur from the proton 'trap' which has been implicated in the protonmotive mechanism [45] so that the $P_M/F^{\cdot}$ change would hence

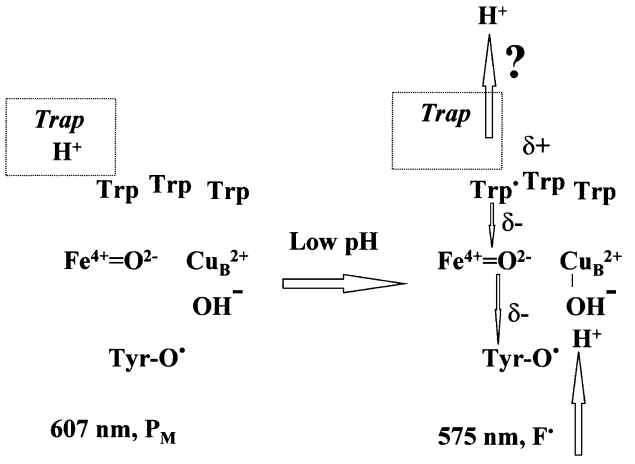

Fig. 7. Possible interrelation of P_M and $F^{\cdot}$. The 607 nm P_M form is assumed to be a ferryl species together with a neutral tyrosine radical that is EPR-silent and, probably, a hydroxide ligand on Cu_B (cf. Ref. [50]). Low pH causes conversion to $F^{\cdot}$ due to protonation close to the tyrosine/hydroxide groups and this in turn causes a partial electron redistribution towards the tyrosine radical and away from the tryptophan(s) close to the binuclear centre. If the overall reaction does not involve a net proton uptake (see Discussion), then protonation of the tyrosine/hydroxide is likely to be coupled to deprotonation from the proton trap site [45], which has been proposed to be close to the binuclear centre towards the positive phase.

simulate a net proton translocation across the membrane (cf. Ref. [50]), as illustrated in Fig. 7. This would further suggest that the proton translocations that are coupled to the reaction cycle need not be rigidly fixed to individual redox states of the reaction cycle: specifically, a reaction cycle proceeding at low pH via $F^{\cdot}$ would have translocated one proton in reaching $F^{\cdot}$, whereas one proceeding at higher pH via the alternative isopotential P_M form would translocate protons only after this stage. Hence, although the full reaction cycle would still involve four proton translocations in both cases and so remains constant in its coupling efficiency, the steps at which the coupled proton translocations occur would not be the same. This very important likelihood has not been addressed previously.

Acknowledgements

This work was supported by grants from the Wellcome Trust (to PR, grant number 062827) and the European Union (to PH, TMR programme Contract No. FMRX-CT98-0214) and was aided by the expert technical support of Mr. Jonathan Ramsey.

References

[1] T. Tsukihara, H. Aoyama, E. Yamashita, T. Tomizaki, H. Yamaguchi, K. Shinzawa-Itoh, R. Nakashima, R. Yaono, S. Yoshikawa, The whole structure of the 13-subunit oxidized cytochrome *c* oxidase at 2.8 Å, Science 272 (1996) 1136–1144.

[2] S. Iwata, C. Ostermeier, B. Ludwig, H. Michel, Structure at 2.8 Å resolution of cytochrome *c* oxidase from *Paracoccus denitrificans*, Nature 376 (1995) 660–669.

[3] G.T. Babcock, M. Wikström, Oxygen activation and the conservation of energy in cell respiration, Nature 356 (1992) 301–309.

[4] M. Wikström, Energy-dependent reversal of the cytochrome oxidase reaction, Proc. Natl. Acad. Sci. U. S. A. 78 (1981) 4051–4054.

[5] M. Wikström, J.E. Morgan, The dioxygen cycle. Spectral, kinetic, and thermodynamic characteristics of ferryl and peroxy intermediates observed by reversal of the cytochrome oxidase reaction, J. Biol. Chem. 267 (1992) 10266–10273.

[6] J.E. Morgan, M.I. Verkhovsky, M. Wikstrom, Observation and assignment of peroxy and ferryl intermediates in the reduction of dioxygen to water by cytochrome *c* oxidase, Biochemistry 35 (1996) 12235–12240.

[7] A. Sucheta, K.E. Georgiadis, O. Einarsdóttir, Mechanism of cytochrome *c* oxidase-catalysed reduction of dioxygen to water: evidence for peroxy and ferryl intermediates at room temperature, Biochemistry 36 (1997) 554–565.

[8] J.E. Morgan, M.I. Verkhovsky, A. Puustinen, M. Wikström, Identification of a "peroxy" intermediate in cytochrome bo_3 of *Escherichia coli*, Biochemistry 34 (1995) 15633–15637.

[9] M. Lauraeus, J.E. Morgan, M. Wikström, Peroxy and ferryl intermediates of the quinol-oxidizing cytochrome aa_3 from *Bacillus subtilis*, Biochemistry 32 (1993) 2664–2670.

[10] P.R. Rich, A.J. Moody, Cytochrome *c* oxidase, in: P. Gräber, G. Milazzo (Eds.), Bioelectrochemistry: Principles and Practice, Birkhäuser Verlag, Basel, (1997) 419–456.

[11] M.I. Verkhovsky, J.E. Morgan, M. Wikström, Redox transitions between oxygen intermediates in cytochrome *c* oxidase, Proc. Natl. Acad. Sci. U. S. A. 93 (1996) 12235–12239.

[12] M. Fabian, G. Palmer, The interaction of cytochrome oxidase with hydrogen peroxide: the relationship of compounds P and F, Biochemistry 34 (1995) 13802–13810.

[13] M. Fabian, G. Palmer, Redox state of peroxy and ferryl intermediates in cytochrome *c* oxidase catalysis, Biochemistry 38 (1999) 6270–6275.

[14] N.J. Watmough, M.R. Cheesman, C. Greenwood, A.J. Thomson, Cytochrome *bo* from *Escherichia coli*: reaction of the oxidized enzyme with hydrogen peroxide, Biochem. J. 300 (1994) 469–475.

[15] D.A. Proshlyakov, T. Ogura, K. Shinzawa-Itoh, S. Yoshikawa, E.H. Appelman, T. Kitagawa, Selective resonance Raman observation of the "607 nm" form generated in the reaction of oxidized cytochrome *c* oxidase with hydrogen peroxide, J. Biol. Chem. 269 (1994) 29385–29388.

[16] D.A. Proshlyakov, T. Ogura, K. Shinzawa-Itoh, S. Yoshikawa, T. Kitagawa, Microcirculating system for simultaneous determination of Raman and absorption spectra of enzymatic reaction intermediates and its application to the reaction of cytochrome *c* oxidase with hydrogen peroxide, Biochemistry 35 (1996) 76–82.

[17] D.A. Proshlyakov, T. Ogura, K. Shinzawa-Itoh, S. Yoshikawa, T. Kitagawa, Resonance Raman/absorption characterization of the oxo intermediates of cytochrome *c* oxidase generated in its reaction with hydrogen peroxide: pH and H_2O_2 concentration dependence, Biochemistry 35 (1996) 8580–8586.

[18] M. Fabian, W.W. Wong, R.B. Gennis, G. Palmer, Mass spectrometric determination of dioxygen bond splitting in the "peroxy" intermediate of cytochrome *c* oxidase, Proc. Natl. Acad. Sci. U. S. A. 96 (1999) 13114–13117.

[19] B. Chance, C. Saronio, J.S. Leigh, Functional intermediates in the reaction of membrane-bound cytochrome oxidase with oxygen, J. Biol. Chem. 250 (1975) 9226–9237.

[20] P. Nicholls, G.A. Chanady, Interactions of cytochrome aa_3 with oxygen and carbon monoxide. The role of the 607 nm complex, Biochim. Biophys. Acta 634 (1981) 256–265.

[21] M.I. Verkhovsky, J.E. Morgan, M. Wikström, Oxygen binding and activation: early steps in the reaction of oxygen with cytochrome *c* oxidase, Biochemistry 33 (1994) 3079–3086.

[22] P. Ädelroth, M. Ek, P. Brzezinski, Factors determining electron-transfer rates in cytochrome *c* oxidase: investigation of the oxygen reaction in the *R. sphaeroides* enzyme, Biochim. Biophys. Acta 1367 (1998) 107–117.

[23] A. Sucheta, I. Szundi, O. Einarsdóttir, Intermediates in the reaction of fully reduced cytochrome *c* oxidase with dioxygen, Biochemistry 37 (1998) 17905–17914.

[24] M. Karpefors, P. Ädelroth, A. Namslauer, Y. Zhen, P. Brzezinski, Formation of the "peroxy" intermediate in cytochrome *c* oxidase is associated with internal proton/hydrogen transfer, Biochemistry 39 (2001) 14664–14669.

[25] J.E. Morgan, M.I. Verkhovsky, G. Palmer, M. Wikström, The role of the P_R intermediate in the reaction of cytochrome *c* oxidase with O_2, Biochemistry 40 (2001) 6882–6892.

[26] J.M. Wrigglesworth, Formation and reduction of a 'peroxy' intermediate of cytochrome *c* oxidase by hydrogen peroxide, Biochem. J. 217 (1984) 715–719.

[27] L. Weng, G.M. Baker, Reaction of hydrogen peroxide with the rapid form of resting cytochrome oxidase, Biochemistry 30 (1991) 5727–5733.

[28] S. Jünemann, P. Heathcote, P.R. Rich, The reactions of hydrogen peroxide with bovine cytochrome *c* oxidase, Biochim. Biophys. Acta 1456 (2000) 56–66.

[29] T. Brittain, R.H. Little, C. Greenwood, N.J. Watmough, The reaction of *Escherichia coli* cytochrome *bo* with H_2O_2: evidence for the formation of an oxoferryl species by two distinct routes, FEBS Lett. 399 (1996) 21–25.

[30] A.J. Moody, P.R. Rich, The reaction of hydrogen peroxide with pulsed cytochrome *bo* from *Escherichia coli*, Eur. J. Biochem. 226 (1994) 731–737.

[31] S.E.J. Rigby, S. Jünemann, P.R. Rich, P. Heathcote, The reaction of hydrogen peroxide with bovine cytochrome *c* oxidase produces a tryptophan cation radical and a porphyrin cation radical, Biochemistry 39 (2000) 5921–5928.
[32] F. MacMillan, A. Kannt, J. Behr, T. Prisner, H. Michel, Direct evidence for a tyrosine radical in the reaction of cytochrome *c* oxidase with hydrogen peroxide, Biochemistry 38 (1999) 9179–9184.
[33] S. Yoshikawa, K. Shinzawa-Itoh, R. Nakashima, R. Yaono, E. Yamashita, N. Inoue, M. Yao, M.J. Fei, C.P. Libeu, T. Mizushima, H. Yamaguchi, T. Tomizaki, T. Tsukihara, Redox-coupled crystal structural changes in bovine heart cytochrome *c* oxidase, Science 280 (1998) 1723–1729.
[34] C. Ostermeier, A. Harrenga, U. Ermler, H. Michel, Structure at 2.7 Å resolution of the *Paracoccus denitrificans* two-subunit cytochrome *c* oxidase complexed with an antibody F_v fragment, Proc. Natl. Acad. Sci. U. S. A. 94 (1997) 10547–10553.
[35] D.M. Mitchell, P. Ädelroth, J.P. Hosler, J.R. Fetter, P. Brzezinski, M.A. Pressler, R. Aasa, B.G. Malmström, J.O. Alben, G.T. Babcock, R.B. Gennis, S. Ferguson-Miller, A ligand-exchange mechanism of proton pumping involving tyrosine −422 of subunit I of cytochrome oxidase is ruled out, Biochemistry 35 (1996) 824–828.
[36] H. Michel, Proton pumping by cytochrome *c* oxidase, Nature 402 (1999) 602–603.
[37] D.A. Proshlyakov, M.A. Pressler, C. DeMaso, J.F. Leykam, D.L. DeWitt, G.T. Babcock, The missing link in cytochrome oxidase: Y_{244} is redox-active in O_2 activation and reduction, Science 290 (2000) 1588–1591.
[38] T. Uchida, T. Mogi, T. Kitagawa, Resonance Raman studies of oxo intermediates in the reaction of pulsed cytochrome *bo* with hydrogen peroxide, Biochemistry 39 (2000) 6669–6678.
[39] A.J. Moody, C.E. Cooper, P.R. Rich, Characterisation of 'fast' and 'slow' forms of bovine heart cytochrome *c* oxidase, Biochim. Biophys. Acta 1059 (1991) 189–207.
[40] D.L. Williams-Smith, P. Heathcote, C.K. Sihra, M.C.W. Evans, Quantitative electron-paramagnetic-resonance measurements of the electron-transfer components of the Photosystem I reaction centre, Biochem. J. 170 (1978) 365–372.
[41] R. Mitchell, P. Mitchell, P.R. Rich, Protonation states of the catalytic cycle intermediates of cytochrome *c* oxidase, Biochim. Biophys. Acta 1101 (1992) 188–191.
[42] C. Pecoraro, R.B. Gennis, T.V. Vygodina, A.A. Konstantinov, Role of the K-channel in the pH-dependence of the reaction of cytochrome *c* oxidase with hydrogen peroxide, Biochemistry 40 (2001) 9695–9708.
[43] D.A. Proshlyakov, M.A. Pressler, G.T. Babcock, Dioxygen activation and bond cleavage by mixed-valence cytochrome *c* oxidase, Proc. Natl. Acad. Sci. U. S. A. 95 (1998) 8020–8025.
[44] R.B. Gennis, Multiple proton-conducting pathways in cytochrome oxidase and a proposed role for the active-site tyrosine, Biochim. Biophys. Acta 1365 (1998) 241–248.
[45] P.R. Rich, Towards an understanding of the chemistry of oxygen reduction and proton translocation in the iron–copper respiratory oxidases, Aust. J. Plant Physiol. 22 (1995) 479–486.
[46] M. Fabian, G. Palmer, Proton involvement in the transition from the "peroxy" to the ferryl intermediate of cytochrome *c* oxidase, Biochemistry 40 (2001) 1867–1874.
[47] N. Capitanio, T.V. Vygodina, G. Capitanio, A.A. Konstantinov, P. Nicholls, S. Papa, Redox-linked protolytic reactions in soluble cytochrome *c* oxidase from beef-heart mitochondria: redox Bohr effects, Biochim. Biophys. Acta 1318 (1997) 255–265.
[48] G.M. Baker, G. Palmer, Effect of high pH on the spectral and catalytic properties of beef heart cytochrome oxidase, Biochemistry 26 (1987) 3038–3044.
[49] A.J. Moody, 'As prepared' forms of fully oxidised haem/Cu terminal oxidases, Biochim. Biophys. Acta 1276 (1996) 6–20.
[50] H. Michel, Cytochrome *c* oxidase: catalytic cycle and mechanisms of proton pumping—a discussion, Biochemistry 38 (1999) 15129–15140.